COMPOSITE MODELING FOR THE EFFECTIVE ELASTIC PROPERTIES OF SEMICRYSTALLINE POLYMERS

Said Ahzi, Nadia Bahlouli, Ahmed Makradi and Salim Belouettar

COMPOSITE MODELING FOR THE EFFECTIVE ELASTIC PROPERTIES OF SEMICRYSTALLINE POLYMERS

SAID AHZI, NADIA BAHLOULI, AHMED MAKRADI AND SALIM BELOUETTAR

It is established that upper and lower bounds predict results far apart from each other for the effective elastic properties of semicrystalline polymers such as polyethylene. This is manly due to the high anisotropy of the elastic properties of the crystals. Composite modeling has been used to predict intermediate results between the bounds. Here, we show the details of composite modeling based on a two phase inclusion (crystalline lamella and amorphous domain) as the local representative element of a semicrystalline polymer. Three approaches, two composite bounds, and a composite self-consistent model, are used to compute the overall elastic properties. Details of the development of these approaches are given in this paper. We find good agreement between results from these approaches and experimental results for polyethylene.

1. Introduction

Under a nondistorted state, semicrystalline polymer morphology is often presented in the shape of spherulites. Each spherulite is composed of crystalline plates arranged radially and separated by an amorphous domain. The macroscopic mechanical behavior of the spherulitic polymer is assumed to be isotropic. When the material is distorted, the spherulitic morphology disappears, leading to an oriented morphology with privileged directions. This arrangement contributes to the increase in global elastic anisotropy. We note that the elastic stiffness in the chain direction of the crystalline lamellae is very high. This local anisotropy appears at a macroscopic scale in the case of oriented polymers.

One of the current and very important challenges for cost-effective design of new advanced polymers and polymer matrix composites hinges upon the use of advanced computational methods and novel micromechanical models that bridge the gap between different material length scales. Here we consider simplified homogenization techniques based on continuum mechanics where the molecular architecture and molecular weight are not explicitly accounted for. However, their effects are somehow included in the values chosen for the homogenized local properties and in the volume fractions of the phases.

For the general case of predicting the effective properties of heterogeneous media, such as the two phase composites, there exist several theories that are used as averaging schemes. For instance, the asymptotic method proposed by [Berlyand and Kozlov 1992; Berlyand and Promislow 1995] can be used to predict the asymptotic behavior of the effective elastic properties of a two phase composite material as the ratio δ of the moduli for the soft (matrix) and hard (inclusion) phases tends to zero ($\delta \to 0$). This asymptotic method has been used to design both isotropic and orthotropic composite materials with particular elastic properties. Among other widely used theories are the Hashin–Shtrikman bounds

[1963], the Mori–Tanaka approach [Mori and Tanaka 1973; Benveniste 1987], the Ponte Castaneda–Willis approach [1995], the double inclusion theory [Hori and Nemat-Nasser 1993; Hu and Weng 2000; Aboutajeddine and Neale 2005] and the statistical approach [Lin and Garmestani 2000; Jefferson et al. 2005]. Specific application of these approaches to semicrystalline polymers is yet to be done to compare results for these materials. While this is an important task, it is out of the scope of the present work, in which we discuss simpler methods.

To calculate the mechanical properties of semicrystalline polymers, Takayanagi et al. [1966] considered the two polymer phases as oriented crystalline blocks alternating with an amorphous phase. This simple model was used to predict the tensile moduli parallel and perpendicular to the draw direction. Another model, proposed by Barham and Arridge [1977], considers the composite nature of the semicrystalline polymer. These two models are used and discussed in [Ward 1985]. Wang [1973] proposed a composite model based on the self-consistent approach of [Hill 1964; 1965; Hermans 1967]. To predict the elastic constant for transcrystalline polyethylene using Hertman's formulation, [Wang 1973] considered transcrystalline polyethylene as crystalline fibers embedded in an isotropic amorphous matrix.

Ahzi et al. [1995] showed that the classical upper and lower bounds result in estimates far apart from each other for elastic isotropic polyethylene (PE), and that the results of [Wang 1973] for transcrystalline PE are very close to those predicted by the classical upper bound. They also suggested the use of two-phase composite inclusion-based modeling to develop intermediate estimates of the elastic properties of semicrystalline polymer. However, some of the details of the intermediate modeling approach were not given in [Ahzi et al. 1995].

Molecular weight is not explicitly accounted for in our present proposed approach. It is well established that small-strain tensile deformation properties, such as Young's modulus, yield stress, and yield strain are directly related to percent crystallinity, independently of molecular weight; [Jordens et al. 2000]. However for low and medium density, Nakayama et al. [1991] and Capaccio et al. [1976] have shown that the crystallinity decreases with increasing molecular weight of PE. This is the case for PE processed following the standard procedure based on slow cooling from the melt, according to this last reference. For instance, the thickness of the amorphous domains is directly related to the square root of molecular weight [Flory 1969]. Under these conditions the crystalline PE has an orthorhombic structure, but when PE is processed under high pressure, a hexagonal crystalline phase is obtained [de Langen et al. 2000]. In the present work we consider PE obtained by slow cooling, where the crystalline phase can be considered as entirely orthorhombic [Addiego et al. 2006]. In our approach, the percent of crystallinity is imposed and therefore the corresponding molecular weight is implicitly accounted for. For other processing procedures where the link between crystallinity and molecular weight may not be so simple, our approach should be modified. This can be done by introducing the molecular weight effect directly in the expression of the local properties. Averaging will therefore account for the effect of molecular weight. However, this point is out of the scope of the current paper.

The present work is based on the composite model of [Ahzi et al. 1995], where the following hypotheses are considered: the elementary representative volume of a semicrystalline polymer is considered as a two-phase composite inclusion representing a crystalline plate and the neighboring amorphous domain. These composite inclusions can be modeled as an extended sandwich with an infinite planar interface (Figure 1). We give the details of the development of three composite models: composite upper bound,
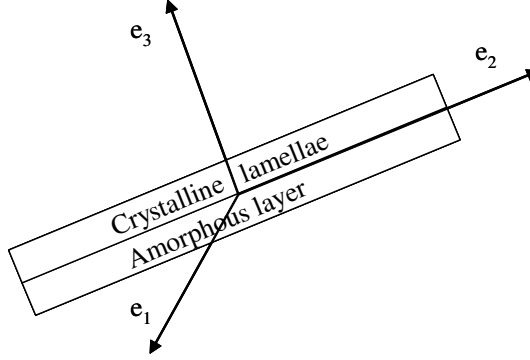
Figure 1. Two-phase composite inclusion.

composite lower bound and composite self-consistent model. To illustrate the result of these intermediate models, we applied them to predict the elastic properties of spherulitic polyethylene. We also compare these results to experimental ones from the literature. These comparisons show that the developed intermediate models give good bounding of experimental results for different crystallinities.

2. Local elastic properties

The elastic constants of the crystals of polyethylene (PE) used in this work are computed in [Zehnder et al. 1996] using atomistic simulations. These elastic constants are expressed in the orthonormal axis of the orthorhombic unit cell of PE crystals as follows:

$$\boldsymbol{C}^c = \begin{bmatrix} 8.50 & 5.00 & 4.50 & 0.00 & 0.00 & 0.00 \\ 5.00 & 9.00 & 6.40 & 0.00 & 0.00 & 0.00 \\ 4.50 & 6.40 & 250.00 & 0.00 & 0.00 & 0.00 \\ 0.00 & 0.00 & 0.00 & 2.80 & 0.00 & 0.00 \\ 0.00 & 0.00 & 0.00 & 0.00 & 1.70 & 0.00 \\ 0.00 & 0.00 & 0.00 & 0.00 & 0.00 & 3.40 \end{bmatrix} \text{GPa},$$

$$\boldsymbol{S}^c = (\boldsymbol{C}^c)^{-1} = \begin{bmatrix} 0.17 & -0.09 & -0.0006 & 0.00 & 0.00 & 0.00 \\ -0.09 & 0.16 & -0.0025 & 0.00 & 0.00 & 0.00 \\ -0.0006 & -0.0025 & 0.004 & 0.00 & 0.00 & 0.00 \\ 0.00 & 0.00 & 0.00 & 0.35 & 0.00 & 0.00 \\ 0.00 & 0.00 & 0.00 & 0.00 & 0.58 & 0.00 \\ 0.00 & 0.00 & 0.00 & 0.00 & 0.00 & 0.29 \end{bmatrix} \text{GPa}^{-1}.$$

For the amorphous phase, since polyethylene (PE) is rubbery at room temperature, atomistic simulations cannot be used to compute the elastic properties. However, Gray and McCrum [1969] reported a Poisson ratio $\nu = 0.49$ and a shear modulus $G^a = 0.1$ GPa for polyethylene. The shear modulus appears to be two orders of magnitude higher than what one would expect for the rubbery phase of PE. This is due to the fact that the measured value is influenced by the presence of the crystalline phase. In the applications shown in this work, we will keep $\nu = 0.49$ and shear modulus $G^a = 0.1$ GPa. As one would
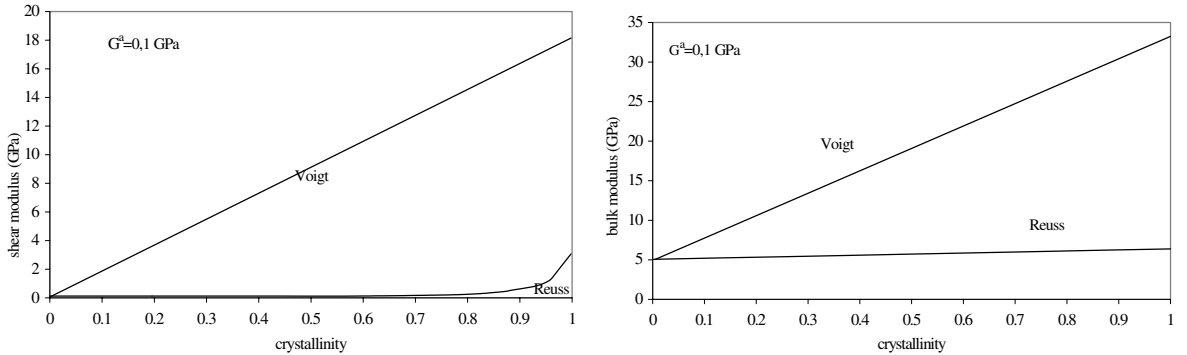
Figure 2. Classical bounds for the shear modulus (left) and bulk modulus (right) for isotropic PE.

expect, the amorphous domains in semicrystalline polymers will not have the same properties as the corresponding bulk material.

3. Classical upper and lower bounds (Voigt and Reuss)

For a semicrystalline polymer with a volume fraction f_a of the amorphous phase, the classical bounds, Voigt (upper bound) and Reuss (lower bound), can be used to compute the effective (average) elastic properties. The Voigt model assumes the uniformity of strain in the material which leads to the expression

$$\boldsymbol{C}^{\text{eff}} = \left\langle f_a \boldsymbol{C}^a + (1 - f_a) \boldsymbol{C}^c \right\rangle \tag{1}$$

for the effective stiffness tensor. The Reuss model assumes uniformity of the stress which yields the expression

$$\boldsymbol{S}^{\text{eff}} = \left\langle f_a \boldsymbol{S}^a + (1 - f_a) \boldsymbol{S}^c \right\rangle \tag{2}$$

for the effective compliance tensor. Here, $\langle \cdot \rangle$ represents the volume average over the aggregate. These classical bounds were implemented in [Ahzi et al. 1995] to predict the effective elastic properties of polyethylene with isotropic distribution of the crystalline lamellae, which represent a spherulitic morphology of polyethylene. The analytical integration procedure for isotropic distribution is outlined in Appendix A. The predicted effective isotropic properties are shown in Figure 2, which depicts the evolution of the shear and bulk moduli as functions of the crystallinity of PE. These results show a very large gap between the predictions of the Voigt and the Reuss models for increasing values of crystallinity. This gap is due to the high anisotropy of the crystalline phase and the fact that these classical models account for the composite nature of semicrystalline polymers, such as PE, only through the volume fraction of the two phases. The wide gap between the two model predictions makes it difficult to consider the classical bounds for accurate predictions of the elastic properties of semicrystalline polymers. Polyethylenes usually have crystallinities ranging from 0.3 to 0.8 and for this range the gap between the curves is too wide to make an estimate of the actual values of the macroscopic elastic properties. As seen in the next section, the development of new composite bounds ensures that the gap between these new bounds is drastically reduced compared to the classical bounds, and hence more accurate predictions of the elastic properties can be made.

4. Proposed composite modelling

Composite inclusion model. The morphology of semicrystalline polymers may be thought of as an assemblage of two-phase inclusions. Each inclusion consists of a crystalline lamella and an adjacent amorphous layer as shown in Figure 1 (see also [Ahzi et al. 1990; Ahzi et al. 1995] and [Lee et al. 1993]). The inclusions are of high aspect ratio and are modeled as infinitely extended planar structures with planar interface between the crystalline and the amorphous phase. Lamellar twist is neglected and linear elasticity is assumed for each individual phase as well as for the composite inclusion and the matrix. Let σ^c, σ^a, and σ^I be the Cauchy stress tensors of the crystalline phase, amorphous phase and the inclusion respectively and let ε^c, ε^a and ε^I be the corresponding infinitesimal elastic strain tensors. The constitutive relation for each phase as well as for the composite inclusion may be written as follows:

Crystalline lamella.

$$\sigma^c = C^c \varepsilon^c \qquad \text{or} \qquad \varepsilon^c = S^c \sigma^c, \tag{3}$$

Crystalline lamella.

$$\sigma^a = C^a \varepsilon^a \qquad \text{or} \qquad \varepsilon^a = S^a \sigma^a, \tag{4}$$

Crystalline lamella.

$$\sigma^I = C^I \varepsilon^I \qquad \text{or} \qquad \varepsilon^I = S^I \sigma^I. \tag{5}$$

Here C^c, C^a, nad C^I represent the fourth order stiffness tensors for the crystalline lamella, the amorphous domain and the composite inclusion respectively, and S^c, S^a, S^I are the corresponding compliance tensors (the inverses of the stiffness tensors). The inclusion stress and strain may be obtained by the volume average of the constituent's stress and strain fields

$$\sigma^I = f_a \sigma^a + (1 - f_a) \sigma^c, \tag{6}$$

and

$$\varepsilon^I = f_a \varepsilon^a + (1 - f_a) \varepsilon^c, \tag{7}$$

where f_a is the volume fraction of the amorphous phase, assumed to be the same for all inclusions.

Interface compatibility and equilibrium. Let us first define the vector form of the stress and strain tensors. These tensors can be expressed as

$$\sigma \equiv \left(\sigma_{11}, \sigma_{22}, \sigma_{33}, \sigma_{23}, \sigma_{13}, \sigma_{12}\right)^T \equiv \left(\sigma_1, \sigma_2, \sigma_3, \sigma_4, \sigma_5, \sigma_6\right)^T, \tag{8}$$

and

$$\varepsilon \equiv \left(\varepsilon_{11}, \varepsilon_{22}, \varepsilon_{33}, \varepsilon_{23}, \varepsilon_{13}, \varepsilon_{12}\right)^T \equiv \left(\varepsilon_1, \varepsilon_2, \varepsilon_3, \varepsilon_4, \varepsilon_5, \varepsilon_6\right)^T, \tag{9}$$

where the superscript T designates the transpose.

The interface between the crystalline and the amorphous phase of each inclusion requires the enforcement of the compatibility and equilibrium conditions. Considering an orthonormal basis (e_1, e_2, e_3) with e_3 normal to the interface and (e_1, e_2) in the plane of the interface, we can then write the strain compatibility at the interface as

$$\varepsilon_\alpha^c = \varepsilon_\alpha^a = \varepsilon_\alpha^I. \tag{10}$$

Here α takes the values 1, 2 and 6. This means that the in-plane strains are continuous across the interface. The stress equilibrium conditions ensure interface traction equilibrium. These conditions are represented by

$$\sigma_\beta^c = \sigma_\beta^a = \sigma_\beta^I. \tag{11}$$

Here β takes the value 3, 4 and 5.

Now the problem is to determine the expressions for C^I and S^I from the stiffness and compliance tensors of the individual phases. From Equations (3), (4), and (5) we note that, to get the expression for the inclusion stiffness and compliance tensors, we need to express σ^a and σ^c in terms of σ^I, and ε^a and ε^c in terms of ε^I. From the above linear relations, we show (see Appendix B) that the phase stress and strain tensors are linearly related to the inclusion stress and strain tensors, respectively. These relations are given by

$$\sigma^a = R^a \sigma^I, \qquad \text{and} \qquad \sigma^c = R^c \sigma^I \tag{12}$$

$$\varepsilon^a = Q^a \varepsilon^I \qquad \text{and} \qquad \varepsilon^c = Q^c \varepsilon^I. \tag{13}$$

The fourth order tensors Q^a, Q^c, R^a and R^c depend on the elastic moduli of the phases. These mapping tensors are termed phase concentration tensors and the analytical determination of their expressions are given in Appendix B.

Inclusion elastic constants. Introducing the constitutive relations given by (3), (4) and (5) in Equation (6) we obtain

$$C^I \varepsilon^I = f_a C^a \varepsilon^a + (1 - f_a) C^c \varepsilon^c, \tag{14}$$

and the use of (12) in (13) leads to

$$C^I \varepsilon^I = \left[f_a C^a Q^a + (1 - f_a) C^c Q^c \right] \varepsilon^I. \tag{15}$$

Thus, the inclusion stiffness tensor is obtained as

$$C^I = f_a C^a Q^a + (1 - f_a) C^c Q^c. \tag{16}$$

Similarly, introducing the constitutive relations (3), (4), and (5) in (7) we obtain

$$S^I \sigma^I = f_a S^a \sigma^a + (1 - f_a) S^c \sigma^c. \tag{17}$$

If the relations of (12) are used in (17), we obtain

$$S^I \sigma^I = \left[f_a S^a R^a + (1 - f_a) S^c R^c \right] \sigma^I. \tag{18}$$

Thus, the inclusion compliance tensor is obtained as

$$S^I = f_a S^a R^a + (1 - f_a) S^c R^c. \tag{19}$$

We note that the expression (19) for the composite inclusion elastic constants is dual to Equation (16): $C^I = (S^I)^{-1}$. However, Voigt-type inclusion-averaging, C^I_{Voigt}, is obtained by setting Q^a and Q^c to identity in relation (16). Reuss-type inclusion averaging, S^I_{Reuss}, is also obtained by setting R^a and R^c to identity in relation (19).
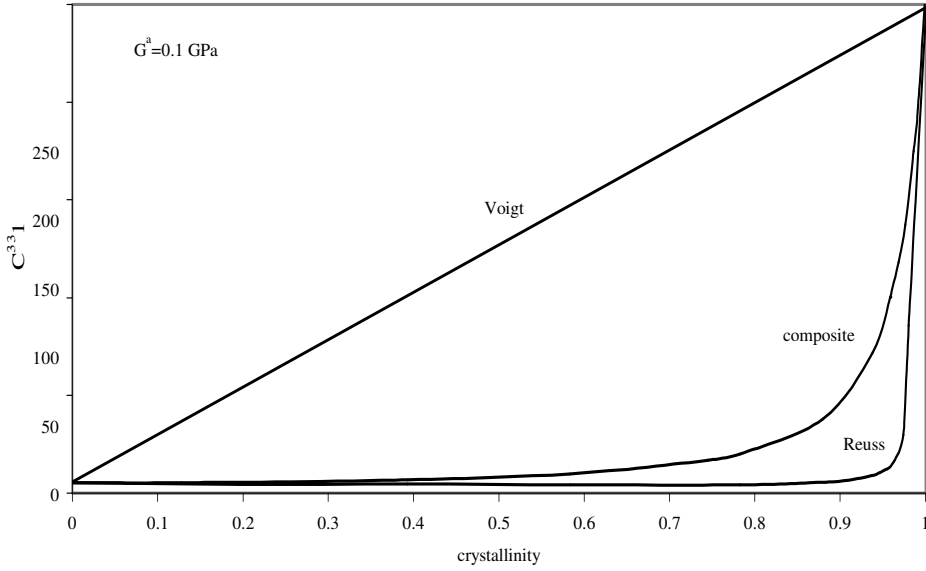
Figure 3. Inclusion stiffness C_{33}^I component.

The stiffness matrix C^I is an important indicator regarding the elastic constants of bulk crystalline polymers such as polyethylene. If we assume the chain direction of the crystalline lamella to be parallel to the inclusion interface normal (e_3), the C_{33}^I element of the inclusion stiffness matrix reflects the variation of local elastic stiffness with crystallinity. Figure 3 shows the variation of this stiffness component as function of crystallinity for the three local averaging schemes discussed above: $C^I_{\text{Composite}}$, C^I_{Voigt}, and $C^I_{\text{Reuss}} = (S^I_{\text{Reuss}})^{-1}$.

Composite averaging schemes. The overall (effective) elastic properties of an aggregate consisting of N inclusions is obtained by averaging the local elastic properties. We consider an aggregate of volume V subjected to a remote macroscopic stress tensor $\bar{\sigma}$ and to the corresponding macroscopic elastic strain tensor $\bar{\varepsilon}$. Considering the overall behavior to be linear elastic, Hooke's law is then given by

$$\bar{\sigma} = C^{\text{eff}}\bar{\varepsilon} \qquad \text{or} \qquad \bar{\varepsilon} = S^{\text{eff}}\bar{\sigma}, \tag{20}$$

where C^{eff} and S^{eff} are the effective stiffness and compliance tensors of the aggregate, respectively. The consistency condition dictates that the average of the local stresses and strains should equal the macroscopic ones, that is

$$\bar{\sigma} = \langle \sigma^I \rangle \equiv \frac{1}{V} \int \sigma^I dV, \tag{21}$$

and

$$\bar{\varepsilon} = \langle \varepsilon^I \rangle \equiv \frac{1}{V} \int \varepsilon^I dV. \tag{22}$$

To obtain an expression for the effective elastic constants as a function of the local ones, we need to apply an interaction law which consists of a relationship between the macroscopic stress (or strain) tensors. This will depend upon the type of averaging scheme chosen.

Composite lower bound. The lower bound estimate assumes stress uniformity within the aggregate. To extend this model to our composite approach, we assume the composite-inclusion stress to be uniform, and the macroscopic stress $\bar{\sigma}$ to be

$$\sigma^I = \bar{\sigma}. \tag{23}$$

Note that the stress in each phase σ^a and σ^c are not necessarily equal to $\bar{\sigma}$. Substituting (23) in (5) we obtain

$$\varepsilon^I = S^I \bar{\sigma}. \tag{24}$$

Taking the volume average of this relation leads to

$$\langle \varepsilon^I \rangle = \langle S^I \rangle \bar{\sigma}. \tag{25}$$

By imposing the global condition (22), and the second equation of (20) we obtain the following expression for the effective compliance tensor:

$$S^{\text{eff}} = \langle S^I \rangle. \tag{26}$$

Using the expression (19), the composite lower bound averaging expression (27) can be written as

$$S^{\text{eff}} = \langle S^I \rangle = \langle f_a S^a R^a + (1 - f_a) S^c R^c \rangle. \tag{27}$$

We note that relation (27) reduces to the Reuss estimate given by (2) if the phase concentration tensors R reduce to identity. The effective stiffness tensor is then obtained by inverting the effective compliance tensor:

$$C^{\text{eff}} = (S^{\text{eff}})^{-1}. \tag{28}$$

Composite upper bound. For the composite upper bound estimate, we assume strain uniformity in the aggregate. That is, each composite inclusion is subjected to the same macroscopic strain $\bar{\varepsilon}$

$$\varepsilon^I = \bar{\varepsilon}, \tag{29}$$

which allows ε^a and ε^c to deviate from $\bar{\varepsilon}$. Substituting (29) in the first part of (5) and taking the volume average of the resulting relation we obtain

$$\langle \sigma^I \rangle = \langle C^I \rangle \bar{\varepsilon}. \tag{30}$$

Using the global equilibrium condition (21) and comparing to the first part of (20) we obtain the composite upper bound expression for the effective elastic stiffness tensor

$$C^{\text{eff}} = \langle C^I \rangle. \tag{31}$$

Using (16), relation (33) becomes

$$C^{\text{eff}} = \langle C^I \rangle = \langle f_a C^a Q^a + (1 - f_a) C^c Q^c \rangle. \tag{32}$$

Here again, we note that relation (32) reduces to the Voigt estimate given by (1) if the phase concentration tensors Q reduce to identity The effective compliance tensor for the composite upper bound is then obtained by inverting the effective stiffness tensor, as

$$S^{\text{eff}} = (C^{\text{eff}})^{-1}. \tag{33}$$

Self-consistent estimate. In our proposed composite bounds, partial local compatibility and equilibrium are satisfied. This is due to the composite inclusion interface conditions given by (10) and (11). To develop a composite self-consistent scheme, we propose to use the two-phase composite inclusion as the local representative element with an elliptical shape, and embedded in infinite homogeneous equivalent medium. To derive the self-consistent interaction law, we use the integral equation method for which details are given in Appendix C. This treatment is analogous to the work of [Zeller and Dederichs 1973], where the Green function method is used to define the integral equation linking local velocity gradient to the macroscopic one. The interaction law obtained by this scheme, in terms of the inclusion versus the macroscopic strain (or stress) tensors, can be expressed by one of the two following dual expressions (see Appendix C):

$$\boldsymbol{\varepsilon}^I = \boldsymbol{B}^I \langle \boldsymbol{B}^I \rangle^{-1} \bar{\boldsymbol{\varepsilon}} \qquad \text{or} \qquad \boldsymbol{\sigma}^I = \boldsymbol{A}^I \bar{\boldsymbol{\sigma}}. \tag{34}$$

Here the fourth order strain-concentration tensor, $\boldsymbol{B}^I$, and the stress-concentration tensor $\boldsymbol{A}^I$ depend on the effective elastic constants, the inclusion elastic constants, and the shape of the inclusion. Because of the normalization procedure used in the development of the self-consistent scheme (see (Appendix C), the consistency conditions (21) and (22) are trivially satisfied by the interaction law (34).

If we insert (34) in the first equation of (5) we obtain

$$\boldsymbol{\sigma}^I = \boldsymbol{C}^I \boldsymbol{B}^I \langle \boldsymbol{B}^I \rangle^{-1} \bar{\boldsymbol{\varepsilon}}. \tag{35}$$

Taking the volume average of (35) and making use of (21), then comparing the final expression with the first equation of (20) leads to the following composite self-consistent expression of the effective stiffness tensor

$$\boldsymbol{C}^{\text{eff}} = \langle \boldsymbol{C}^I \boldsymbol{B}^I \rangle \langle \boldsymbol{B}^I \rangle^{-1}. \tag{36}$$

If we use (16), the above expression becomes

$$\boldsymbol{C}^{\text{eff}} = \langle [f_a \boldsymbol{Q}^a \boldsymbol{C}^a + (1 - f_a) \boldsymbol{Q}^c \boldsymbol{C}^c] \boldsymbol{B}^I \rangle \langle \boldsymbol{B}^I \rangle^{-1}. \tag{37}$$

The self-consistent estimate of the effective compliance tensor can be obtained by inverting the stiffness tensor given by (37). Or, if we use the interaction law given by the second equation of (34) and reasoning similar to that given above, a dual expression to (37) can be obtained as

$$\boldsymbol{S}^{\text{eff}} = \langle (f_a \boldsymbol{R}^a \boldsymbol{S}^a + (1 - f_a) \boldsymbol{R}^c \boldsymbol{S}^c) \boldsymbol{A}^I \rangle. \tag{38}$$

5. Results and discussion

Predicted results for isotropic polyethylene. To illustrate differences between model predictions, we first evaluate the single inclusion elastic constant C_{33}^I as a function of crystallinity. For this, the crystal elastic constants of the polyethylene are computed by [Zehnder et al. 1996] using atomistic simulations (see Section 1), while those for the amorphous phase are calculated using a shear modulus $G^a = 0.1\,\text{GPa}$. In Figure 3, the values of C_{33}^I have been plotted against crystallinity for the Voigt model (Equation (16), with $\boldsymbol{Q}^a = \boldsymbol{Q}^c = \boldsymbol{I}$), Reuss model (as in Equation (19), with $\boldsymbol{R}^a = \boldsymbol{R}^c = \boldsymbol{I}$), and composite inclusion model (Equation (16)). The nature of the curves reflects that the C_{33}^I elastic constant for the Voigt model increases almost linearly as a function of the crystallinity, compared to the composite inclusion and Reuss models. These predicted results show moderate variation of the elastic constant C_{33}^I with the crystallinity for the composite inclusion and Reuss models except for polyethylene with high crystallinity.

Comparisons between models. The predicted results for the effective shear and bulk moduli as a function of crystallinity of isotropic polyethylene are reported in Figure 4. We notice that the gap between the composite inclusion bounds is drastically reduced relative to the classical bounds except for high concentration of the crystalline phase. In fact, the composite inclusion bounds demonstrate dependence of the stiffness of the crystalline and amorphous phases by enforcement of interface compatibility and equilibrium conditions, which result in reduction of the stiffness of the composite inclusion in the chain direction. In contrast, the classical Voigt and Reuss models assume that the crystalline and amorphous phases deform independently. The imposed uniform strain and high stiffness of the crystals in the chain directions are responsible for over-prediction of the elastic properties by the classical Voigt model.

Regarding self-consistent representation based on the composite inclusion-model, the predicted results fall between the composite bounds. At low crystallinity, the self-consistent curves show a closer response
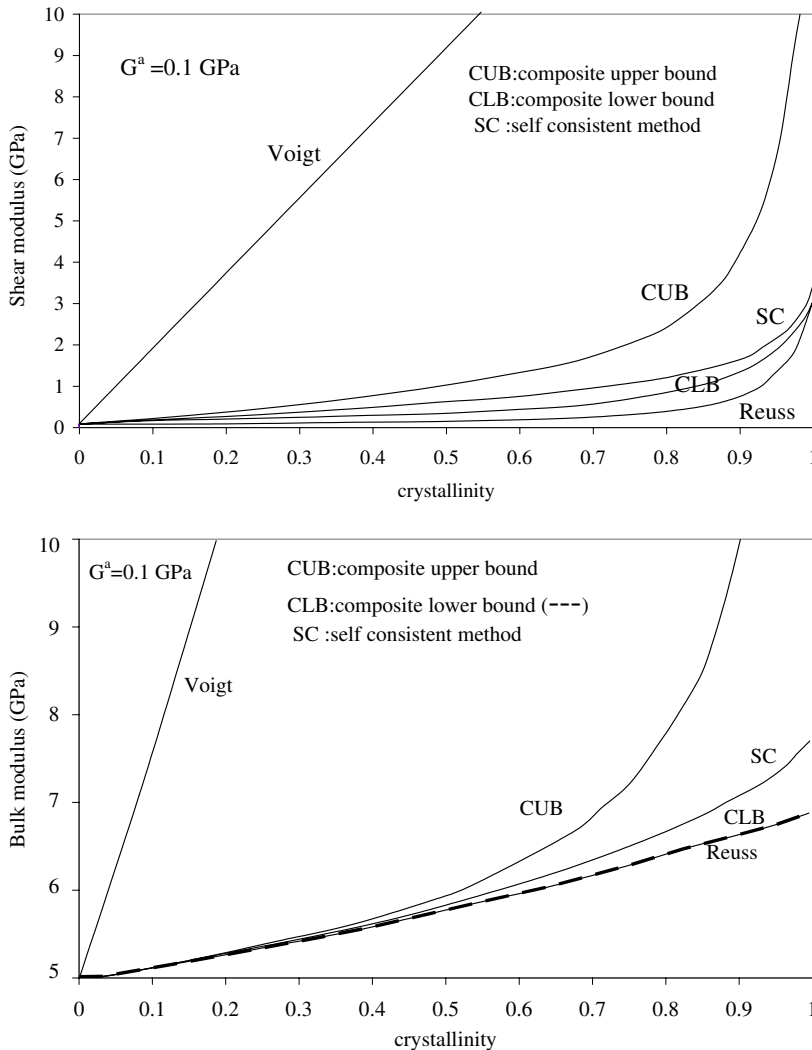

Figure 4. Shear modulus (top) and bulk modulus (bottom) for polyethelyne.

to the composite inclusion lower bound. This behavior is moderately inverted as crystallinity increases but remains in general closer to the composite inclusion lower bound.

Shape effect for the composite self-consistent model. Since the self-consistent approach accounts for inclusion shape effects, in the shear and bulk moduli are reported in Figure 5 for isotropic polyethylene with different inclusion shapes: spherical ($a/c = b/c = 1$), penny-shaped ($a/c = b/c = 5$), and oblate ($a/c = 5$, $b/c = 10$). It can be seen that the predicted elastic properties are very similar for both the penny-shaped and oblate-shaped inclusions. Both the penny and oblate shapes can be used as good inclusion shape approximations of the lamellar structure of polyethylene.

Comparison with experimental results. Davidse et al. [1962] have determined the Young's modulus by measuring the sound velocity, v, and density, ρ, of various polyethylene samples. The Young's modulus
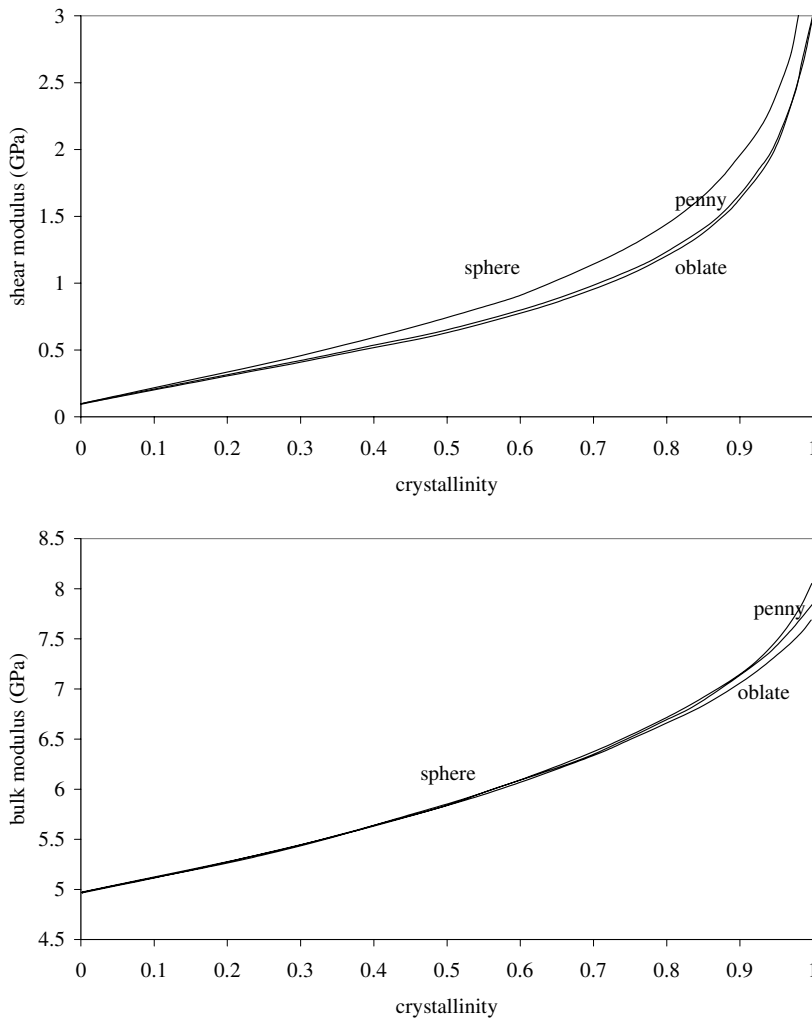

Figure 5. Shear modulus (top) and bulk modulus (bottom) for different inclusion shapes by the self-consistent model.

is related to the sound velocity as

$$E = v^2 \rho. \tag{39}$$

According to [Janzen 1992a; 1992b; 1997], the experimental results of Davidse et al. [1962] cannot be uncritically accepted because their measurements are about three times greater than those obtained from bending and tensile tests. Though this difference was attributed to larger deformations in the bending and tensile tests, the anomaly needs to looked into with a deeper perspective.

[Janzen 1992b] has compared values of the Young's modulus of polyethylene obtained from ultrasound techniques with those obtained from static compression tests. The ultrasound experimental data are from [Hartmann and Jarzynski 1974], while static compression results are taken from [Lagakos et al. 1986].

Experimental data from [Janzen 1992b] and [Davidse et al. 1962] are compared to our predicted results in Figure 6 for the Young's and shear moduli. These results show that the experimental results lie within the composite inclusion bounds.
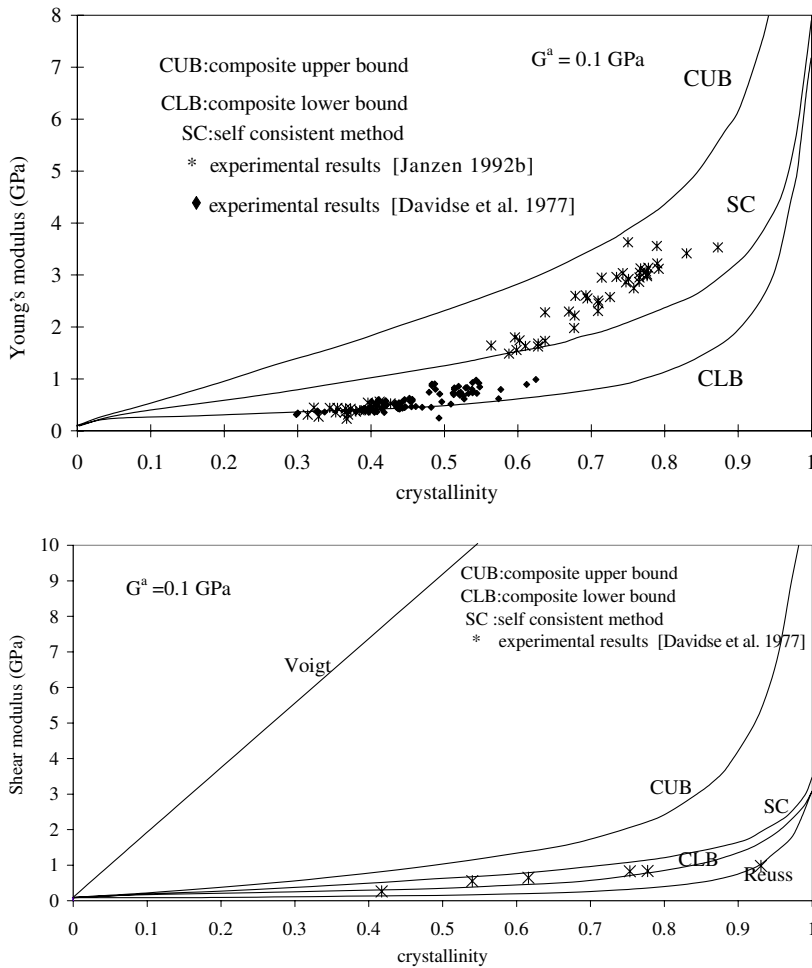

Figure 6. Predicted Young's modulus (left) and shear modulus (right) compared to experimental results of [Janzen 1992b; Davidse et al. 1962].

Conclusion

An averaging scheme for a semicrystalline polymeric material is developed to predict the evolution of the elastic properties function of the crystalline phase volume fraction. The proposed scheme is formulated so as to enforce the local equilibrium and compatibility conditions, which are violated partially by Voigt and Reuss estimates. The classical Voigt and Reuss averaging schemes, where the presence of both crystalline and amorphous phases is represented only by their relative volume fractions, results in far-apart estimates of the effective elastic properties, particularly for the high volume fraction of the crystalline phase. To develop new bounds, the problem of two-phase composite inclusion is considered, where the crystalline and amorphous domains of such a homogenized inclusion are subject to piecewise constant strains and stresses. The satisfaction of interface compatibility and traction equilibrium results in a softer inclusion stiffness, particularly in the crystallographic chain direction. Composite bounds, as well as a self-consistent averaging scheme are used to predict elastic properties of isotropic polyethylene. The composite approach resulted in much narrower difference between the new composite bounds compared to the classical ones. Comparison of predictions of the composite inclusion models with experimental data shows good agreement. We are working on other homogenization approaches for these materials.

An important shortcoming of the proposed modeling is related to the effects of molecular weight and molecular architecture that are ignored. Molecular weight is certainly an important factor that needs to be addressed. In our model, molecular weight is included in a very simple implicit way through the crystallinity and through the chosen values for the local properties. A way to extend the proposed model to include the effect of molecular weight would be to express the crystallinity and local properties as function of the molecular weight. In the modeling proposed here the effect of molecular architecture (that is, linear versus branched chains) cannot be accounted for in an explicit way since the local properties (inputs) are rather homogenized over a local volume. Only molecular simulations can directly account for the effect of molecular architecture. Thus, one way of resolving this would be to combine our modeling with molecular simulations. The latter can be used to compute the local properties as function of molecular architecture then use the results as input for our modeling. We note that for the crystalline phase, the input we used (the elastic properties of the crystalline phase), are those based on atomistic simulations. Here again, the atomistic simulations were conducted on a small volume, which represents only a fraction of the crystalline lamella. In our approach, we have simplified the problem by assuming that these atomistically computed properties are homogeneous within the entire crystalline lamella. Without these simplifying assumptions, no homogenization technique can be developed based on continuum mechanics.

Appendix A. Isotropic distribution

This appendix develops the inclusion average of the stiffness (or compliance), in the case of isotropic distribution of the aggregate such as in spherulitic morphology. If we consider θ, ϕ and Φ to be the Euler angles between the local coordinate system of inclusion and the global coordinate system, we can write the inclusion average of the stiffness (or compliance) as

$$\langle C^I_{ijkl} \rangle = \int_0^{2\pi} \int_0^{2\pi} \int_0^{\pi} a_{ii'}, a_{jj'}, a_{kk'}, a_{ll'}, C^I_{i'j'k'l'} \Phi \sin\theta \, d\theta \, d\phi \, d\psi, \tag{A1}$$

where $\Phi = 1/(8\pi^2)$ and the transform matrix components $a_{ij'}$ are given by

$$a_{11'} = \cos\psi\cos\theta\cos\phi - \sin\psi\sin\phi, \qquad a_{21'} = \cos\psi\cos\theta\sin\phi + \sin\psi\cos\phi, \qquad a_{31'} = -\cos\psi\sin\theta,$$

$$a_{12'} = -\cos\psi\sin\phi - \sin\psi\cos\theta\cos\phi, \qquad a_{22'} = -\sin\psi\cos\theta\sin\phi + \cos\psi\cos\phi, \qquad a_{32'} = \sin\psi\sin\theta,$$

$$a_{13'} = \sin\theta\cos\phi, \qquad a_{23'} = \sin\theta\sin\phi, \qquad a_{33'} = \cos\theta.$$

Carrying out this integration we get the following nonzero components of the symmetric effective stiffness tensor:

$$
\begin{aligned}
C^{\text{eff}} &= \langle C^I \rangle, \\
C_{11}^{\text{eff}} = C_{22}^{\text{eff}} = C_{33}^{\text{eff}} &= \tfrac{1}{15}\big(3(C_{11}^I + C_{22}^I + C_{33}^I) + 2(C_{12}^I + C_{13}^I + C_{23}^I) + 4(C_{44}^I + C_{55}^I + C_{66}^I)\big), \\
C_{12}^{\text{eff}} = C_{23}^{\text{eff}} = C_{13}^{\text{eff}} &= \tfrac{1}{15}\big((C_{11}^I + C_{22}^I + C_{33}^I) + 4(C_{12}^I + C_{13}^I + C_{23}^I) - 2(C_{44}^I + C_{55}^I + C_{66}^I)\big), \\
C_{21}^{\text{eff}} = C_{31}^{\text{eff}} = C_{32}^{\text{eff}} &= C_{12}^{\text{eff}} \\
C_{44}^{\text{eff}} = C_{55}^{\text{eff}} = C_{66}^{\text{eff}} &= \tfrac{1}{15}\big((C_{11}^I + C_{22}^I + C_{33}^I) - (C_{12}^I + C_{13}^I + C_{23}^I) + 3(C_{44}^I + C_{55}^I + C_{66}^I)\big).
\end{aligned}
\tag{A2}
$$

Appendix B. Determination of phase concentration tensors

The phase concentration tensors relate the stress and strain of the phases to the inclusion stress as shown by Equations (10)–(13). We first determine the expression for the tensors $\boldsymbol{Q}^c$ and $\boldsymbol{Q}^a$. In this appendix, the Greek subscripts α and α' take the values 1, 2 and 6, and β and β' take the values 3, 4 and 5. The non-Greek subscripts take all integer values from 1 to 6.

Determination of $\boldsymbol{Q}^c$. The second relation in (13) may be written in component form as

$$\varepsilon_i^c = Q_{ij}^c \varepsilon_j^I, \tag{B1}$$

where the index i and j both range from 1 to 6. For the index $\alpha = 1, 2$, and 6 we can write this equation as

$$\varepsilon_\alpha^c = Q_{\alpha j}^c \varepsilon_j^I. \tag{B2}$$

Using the compatibility condition as given by (9) we can write (B2) as

$$\varepsilon_\alpha^I = Q_{\alpha j}^c \varepsilon_j^I. \tag{B3}$$

Now, when $j = \alpha$, $Q_{\alpha j}^c$ should be equal to identity and when $j \neq \alpha$, $Q_{\alpha j}^c$ should be zero, that is,

$$Q_{\alpha j}^c = \delta_{\alpha j}, \tag{B4}$$

where δ is the Kronecker delta symbol.

To determine the other components of $\boldsymbol{Q}^c$, that is, $Q_{\beta j}$, with $\beta = 3, 4, 5$ we need to consider the equilibrium condition $\sigma_\beta^c = \sigma_\beta^a$ represented by Equation (9). Inserting Hooke's law into this equation we obtain

$$C_{\beta j}^c \varepsilon_j^c = C_{\beta j}^a \varepsilon_j^a. \tag{B5}$$

Equation (5) may be rewritten as

$$\varepsilon_j^a = \frac{1}{f_a}\varepsilon_j^I - \frac{1 - f_a}{f_a}\varepsilon_j^c. \tag{B6}$$

Substituting this in (B5) we obtain

$$\left(C^c_{\beta j} + \frac{1 - f_a}{f_a} C^a_{\beta j} \right) \varepsilon^c_j = \frac{1}{f_a} C^a_{\beta j} \varepsilon^I_j. \tag{B7}$$

This equation can be split into components represented by indices α and β as

$$\left(C^c_{\beta \beta'} + \frac{1 - f_a}{f_a} C^a_{\beta \beta'} \right) \varepsilon^c_{\beta'} + \left(C^c_{\beta \alpha} + \frac{1 - f_a}{f_a} C^a_{\beta \alpha} \right) \varepsilon^c_\alpha = \frac{1}{f_a} C^a_{\beta j} \varepsilon^I_j, \tag{B8}$$

where β' takes the value 3, 4 and 5. Using the compatibility condition $\varepsilon^c_\alpha = \varepsilon^I_\alpha$ as given Equation (8), we obtain

$$\left(C^c_{\beta \beta'} + \frac{1 - f_a}{f_a} C^a_{\beta \beta'} \right) \varepsilon^c_{\beta'} = \frac{1}{f_a} C^a_{\beta j} \varepsilon^I_j - \left(C^c_{\beta \alpha} + \frac{1 - f_a}{f_a} C^a_{\beta \alpha} \right) \delta_{\alpha j} \varepsilon^I_j. \tag{B9}$$

This equation may be written in a more convenient form as

$$H_{\beta \beta'} \varepsilon^c_{\beta'} = K_{\beta j} \varepsilon^I_j, \tag{B10}$$

where

$$H_{\beta \beta'} = C^c_{\beta \beta'} + \frac{1 - f_a}{f_a} C^a_{\beta \beta'} \tag{B11}$$

and

$$K_{\beta j} = \frac{1}{f_a} C^a_{\beta j} - \left(C^c_{\beta \alpha} + \frac{1 - f_a}{f_a} C^a_{\beta \alpha} \right) \delta_{\alpha j}. \tag{B12}$$

From (B10) we get

$$\varepsilon^c_{\beta'} = H^{-1}_{\beta \beta'} K_{\beta j} \varepsilon^I_j. \tag{B13}$$

Comparing with (B1) we deduce

$$Q^c_{\beta j} = H^{-1}_{\beta \beta'} K_{\beta' j}. \tag{B14}$$

Finally, (B4) and (B14) define the tensor $\boldsymbol{Q}^c$ completely.

Determination of $\boldsymbol{Q}^a$. Equation (13) in indicial notation may be written as

$$\varepsilon^a_i = Q^a_{ij} \varepsilon^I_j \tag{B15}$$

again continuity condition (9) implies

$$Q^a_{\alpha j} = \delta_{\alpha j}. \tag{B16}$$

The other components of $Q^a_{\alpha j}$ ie. $Q^a_{\beta j}$ are obtained as follows. Substituting (B1) in (7) we obtain

$$\varepsilon^I_\beta = f_a \varepsilon^a_\beta + (1 - f_a) Q^c_{\beta j} \varepsilon^I_j \tag{B17}$$

or

$$\varepsilon^a_\beta = \frac{1}{f_a} \left(\delta_{\beta j} + (1 - f_a) Q^c_{\beta j} \right) \varepsilon^I_j; \tag{B18}$$

comparing this with (B15) we obtain

$$Q^a_{\beta j} = \frac{1}{f_a} \left(\delta_{\beta j} + (1 - f_a) Q^c_{\beta j} \right). \tag{B19}$$

Therefore, (B16) and (B19) define the tensor $\boldsymbol{Q}^a$ completely. We now determine the phase concentration tensors $\boldsymbol{R}^c$ and $\boldsymbol{R}^a$.

Determination of $\boldsymbol{R}^c$. The second relation in (12) in indicial notation may be written as

$$\sigma_i^c = R_{ij}^c \sigma_i^I. \tag{B20}$$

For $\beta = 3, 4$, and 5 we can write

$$\sigma_\beta^c = R_{\beta j}^c \sigma_j^I. \tag{B21}$$

Using the equilibrium condition (11) leads to

$$R_{\beta j}^a = \delta_{\beta j}. \tag{B22}$$

The remaining components of $\boldsymbol{R}^a$ are determined by considering the compatibility conditions. Introducing Hooke's law into the compatibility equation $\varepsilon_\alpha^c = \varepsilon_\alpha^a$ as given by (10) we obtain

$$S_{\alpha j}^c \sigma_j^c = S_{\alpha j}^a \sigma_j^a. \tag{B23}$$

From (6) and (B23) we obtain

$$\left(S_{\alpha j}^c + \frac{1 - f_a}{f_a} S_{\alpha j}^a\right)\sigma_j^c = \frac{1}{f_a} S_{\alpha j}^a \sigma_j^I. \tag{B24}$$

Splitting this equation into components given by the indices α and β we obtain

$$\left(S_{\alpha\alpha'}^c + \frac{1 - f_a}{f_a} S_{\alpha\alpha'}^a\right)\sigma_{\alpha'}^c + \left(S_{\alpha\beta}^c + \frac{1 - f_a}{f_a} S_{\alpha\beta}^a\right)\sigma_\beta^c = \frac{1}{f_a} S_{\alpha j}^a \sigma_j^I, \tag{B25}$$

where α' takes the value 1, 2 and 6. Using the equilibrium relation $\sigma_\beta^c = \sigma_\beta^I$ as given by (11) we obtain

$$\left(S_{\alpha\alpha'}^c + \frac{1 - f_a}{f_a} S_{\alpha\alpha'}^a\right)\sigma_{\alpha'}^c = \frac{1}{f_a} S_{\alpha j}^a \sigma_j^I - \left(S_{\alpha\beta}^c + \frac{1 - f_a}{f_a} S_{\alpha\beta}^a\right)\delta_{\beta j}\sigma_j^I. \tag{B26}$$

This equation may be written in a more convenient form as

$$L_{\alpha\alpha'}\sigma_{\alpha'}^c = M_{\alpha j}\sigma_j^I, \tag{B27}$$

where

$$L_{\alpha\alpha'} = S_{\alpha\alpha'}^c + \frac{1 - f_a}{f_a} S_{\alpha\alpha'}^a, \tag{B28}$$

and

$$M_{\alpha j} = \frac{1}{f_a} S_{\alpha j}^a - \left(S_{\alpha\beta}^c + \frac{1 - f_a}{f_a} S_{\alpha\beta}^a\right)\delta_{\beta j}. \tag{B29}$$

Thus

$$\sigma_{\alpha'}^c = L_{\alpha\alpha'}^{-1} M_{\alpha j}\sigma_j^I. \tag{B30}$$

Comparing this with Equation (B20) gives

$$R_{\alpha j}^c = L_{\alpha\alpha'}^{-1} M_{\alpha' j}. \tag{B31}$$

Therefore, (B22) and (B31) define the tensor $\boldsymbol{R}^c$.

Determination of R^a. The first relation in (12) in indicial notation may be written as

$$\sigma_i^a = R_{ij}^a \sigma_j^I. \tag{B32}$$

The equilibrium condition (11) implies

$$R_{\beta j}^a = \delta_{\beta j}. \tag{B33}$$

The other components of R_{ij}^a, that is, $R_{\beta j}^a$ are obtained as follows. Substituting (B32) in (6) we obtain

$$\sigma_\beta^I = f_a \sigma_\beta^a + (1 - f_a) R_{\beta j}^c \sigma_j^I, \tag{B34}$$

or

$$\sigma_\beta^a = \frac{1}{f_a} \big(\delta_{\beta j} - (1 - f_a) R_{\beta j}^c \big) \sigma_j^I. \tag{B35}$$

Comparing this with (B32) we obtain

$$R_{\beta j}^a = \frac{1}{f_a} \big(\delta_{\beta j} - (1 - f_a) R_{\beta j}^c \big). \tag{B36}$$

Equations (B33) and (B36) define the tensor $\boldsymbol{R}^a$ completely.

Appendix C. Self-consistent model

In this appendix we develop the self consistent approach applied to semicrystalline polymers. This approach is based on the self-consistent scheme developed in [Zeller and Dederichs 1973] for the elastic properties of polycrystals. Here, we assume small elastic deformations, and that the components of the strain field, ε_{ij}, are defined as the symmetric part of the displacement gradient:

$$\varepsilon_{ij} = \tfrac{1}{2}(u_{i,j} + u_{j,i}) \tag{C1}$$

with

$$u_{i,j} = \frac{\partial u_i}{\partial r_j}, \tag{C2}$$

where the u_i are the components of the displacement vector and the r_j the components of the spatial position vector $\boldsymbol{r}$.

In an elastic material, the stress field is in general dependent on the spatial position $\boldsymbol{r}$, and is related to the strain field ε_{ij} through a local Hooke's law

$$\sigma_{ij} = C_{ijkl}\varepsilon_{kl} \equiv C_{ijkl}u_{k,l}. \tag{C3}$$

The elastic constants are statistically fluctuating quantities which can be decomposed into a sum of a constant part, C_{ijkl}^0, and a fluctuating part, $\tilde{C}_{ijkl}(r)$

$$C_{ijkl} = C_{ijkl}^0 + \tilde{C}_{ijkl}. \tag{C4}$$

The macroscopic homogeneous material is subject to a stress field $\bar{\sigma}_{ij}$, and a corresponding strain field $\bar{\varepsilon}_{ij}$. The elastic constants C_{ijkl}^0 used in the decomposition can be taken as equal to those of the homogeneous equivalent medium, as

$$C_{ijkl}^0 = C_{ijkl}^{\text{eff}}. \tag{C5}$$

The problem consists of finding a solution for the local strain or stress fields as a function of the macroscopic fields. We start by writing the equilibrium

$$\sigma_{ij,j} = C_{ijkl}^{\text{eff}} u_{k,lj} + (\tilde{C}_{ijkl} u_{k,l})_{,j} = 0. \tag{C6}$$

The solution of the Navier equation given by (C6), for given surface displacements $\bar{u}_i^*$, can be written as

$$u_i(\boldsymbol{r}) = \bar{u}_i^*(\boldsymbol{r}) + \int_V G_{ik}(\boldsymbol{r}, \boldsymbol{r}') \big[\tilde{C}_{klmn}(\boldsymbol{r}') u_{m,n}(\boldsymbol{r}')\big]_{,l'} d\boldsymbol{r}', \tag{C7}$$

where V is the volume of the entire aggregate and $G_{kl}(\boldsymbol{r}, \boldsymbol{r}')$ are the components of a Green tensor which satisfies the equilibrium relation

$$C_{ijkl}^{\text{eff}} G_{km,lj}(\boldsymbol{r}, \boldsymbol{r}') + \delta_{im}\delta(\boldsymbol{r} - \boldsymbol{r}') = 0. \tag{C8}$$

It is convenient to assume an infinite medium. This assumption implies the following properties:

$$G_{ij}(\boldsymbol{r}, \boldsymbol{r}') = G_{ij}(\boldsymbol{r} - \boldsymbol{r}') \tag{C9}$$

$$G_{ij,l'} = -G_{ij,l}. \tag{C10}$$

Note that indexes with a prime symbol are relative to $\boldsymbol{r}'$.

By partial integration and subsequent differentiation of (C7) we obtain an integral equation for the local strain tensor

$$\varepsilon_{ij}(\boldsymbol{r}) = \bar{\varepsilon}_{ij}^* + \int_V g_{ijkl}(\boldsymbol{r}, \boldsymbol{r}') \tilde{C}_{klmn}(\boldsymbol{r}') \, \varepsilon_{mn}(\boldsymbol{r}') d^3\boldsymbol{r}', \tag{C11}$$

where

$$g_{ijkl} = \tfrac{1}{4}(G_{ik,jl} + G_{jk,il} + G_{il,jk} + G_{jl,ik}). \tag{C12}$$

We are now looking for an approximate solution of the integral equation (C11). For this, we make use of the Eshelby's solution and proof [1957] of the uniformity of the strain field within an ellipsoidal inclusion embedded in a linear matrix. Our material is represented by N inclusions, and the strain of each of them can be taken as

$$\varepsilon_{ij}^I = \frac{1}{V_I} \int_{V_I} \varepsilon_{ij}(\boldsymbol{r}) d^3\boldsymbol{r}, \tag{C13}$$

where V_I is the volume of the inclusion I. Since the strain is uniform within each inclusion, we have

$$\varepsilon_{ij}(\boldsymbol{r}) = \sum_{I=1}^{N} \varepsilon_{ij}^I \Delta_I(\boldsymbol{r}), \qquad C_{ijkl}(\boldsymbol{r}) = \sum_{I=1}^{N} C_{ijkl}^I \Delta_I(\boldsymbol{r}), \qquad \tilde{C}_{ijkl}(\boldsymbol{r}) = \sum_{I=1}^{N} \tilde{C}_{ijkl}^I \Delta_I(\boldsymbol{r}). \tag{C14}$$

Here, Δ_I is the characteristic function of the inclusion I. It has unit value if $\boldsymbol{r}$ falls within V_I and zero value if not.

If we insert (C13) and (C14) into (C11) and neglect the inclusion-inclusion interaction terms [Molinari et al. 1987], the integral equation (C11) is then approximated by

$$\varepsilon_{ij}^I = \bar{\varepsilon}_{ij}^{*I} + \Gamma_{ijkl} \tilde{C}_{klmn}^I \varepsilon_{mn}^I. \tag{C15}$$

The matrix-inclusion interaction tensor Γ is given by

$$\Gamma_{ijkl} = \frac{1}{V_I} \int_{V_I} \int_{V_I} g_{ijkl} d^3\boldsymbol{r} d^3\boldsymbol{r}'. \tag{C16}$$

Note that the Eshelby tensor is defined as $E_{ijkl} = -\Gamma_{ijmn} C^{\text{eff}}_{mnkl}$.

Finally, a rearrangement of (C15) leads to

$$\varepsilon^I_{ij} = B^I_{ijkl} \bar{\varepsilon}^*_{kl}, \tag{C17}$$

with

$$B^I_{ijkl} = \left[I_{ijkl} - \Gamma_{ijmn} \tilde{C}^I_{mnkl} \right]^{-1}. \tag{C18}$$

At this point, the macroscopic strain $\bar{\boldsymbol{\varepsilon}}^*$ is not specified. The consistency condition requires that the average of local (inclusion) strains should equal the macroscopically imposed strain. If all inclusions of the aggregate have parallel principal axes, this condition is easily met, which also implies that $\bar{\varepsilon}^*$ is exactly the macroscopically imposed strain. However, if the principal axes of the inclusions are not parallel, the consistency condition needs to be enforced using a normalization procedure. For this, we denote by $\bar{\boldsymbol{\varepsilon}}$ the macroscopically imposed strain and assume the relation

$$\bar{\boldsymbol{\varepsilon}}^* = \boldsymbol{K}\bar{\varepsilon}, \tag{C19}$$

where the fourth order tensor K is uniform. If we insert (C19) into (C17) we obtain

$$\langle \boldsymbol{\varepsilon}^I \rangle = \langle \boldsymbol{B}^I \rangle \boldsymbol{K}\bar{\varepsilon}. \tag{C20}$$

Therefore, the consistency condition leads to

$$\boldsymbol{K} = \langle \boldsymbol{B}^I \rangle^{-1}. \tag{C21}$$

The final expression of the interaction law (C17) is given by

$$\boldsymbol{\varepsilon}^I = \boldsymbol{B}^I \langle \boldsymbol{B}^I \rangle^{-1} \bar{\boldsymbol{\varepsilon}}. \tag{C22}$$

Now, if we insert Hooke's law into (C17), a dual interaction law that expresses the inclusion stress $\boldsymbol{\sigma}^I$ as a function of the macroscopic one, $\bar{\boldsymbol{\sigma}}$ can be obtained as

$$\sigma^I_{ij} = A^I_{ijkl} \bar{\sigma}_{kl}, \tag{C23}$$

with

$$A^I = C^I B^I \langle B^I \rangle^{-1} (C^{\text{eff}})^{-1}. \tag{C24}$$

By averaging Equations (C23) and using the estimate given by (36) with relation (C24), one can easily show that $\langle \boldsymbol{A}^I \rangle = \boldsymbol{I}$.

To compute the interaction tensor $\boldsymbol{\Gamma}$ we use the Fourier transform method. Details of the computations may be found in [Ghahremani 1977] and [Gavazzi and Lagoudas 1990].

References

[Aboutajeddine and Neale 2005] A. Aboutajeddine and K. W. Neale, "The double-inclusion model: a new formulation and new estimates", *Mech. Mater.* **37**:2–3 (2005), 331–341.

[Addiego et al. 2006] F. Addiego, A. Dahoun, C. G'Sell, and J. M. Hiver, "Characterization of volume strain at large deformation under uniaxial tension in high-density polyethylene", *Polymer* **47**:12 (2006), 4387–4399.

[Ahzi et al. 1990] S. Ahzi, D. M. Parks, and A. S. Argon, "Modeling of plastic deformation and evolution of anisotropy in semi-crystalline polymers", pp. 287–292 in *Computer modeling and simulation of manufacturing processes: presented at the Winter Annual Meeting of the ASME* (Dallas, TX), edited by B. Singh, ASME, New York, 1990.

[Ahzi et al. 1995] S. Ahzi, D. Parks, and A. Argon, "Estimates of the overall elastic properties in semi-crystalline polymers", pp. 31–44 in *Current research in the thermo-mechanics of polymers in the rubbery-glassy range* (Los Angeles), edited by M. Negahban, Applied Materials Division **203**, ASME, New York, 1995.

[Barham and Arridge 1977] P. J. Barham and R. G. C. Arridge, "Fiber composite model of highly oriented polyethylene", *J. Polym. Sci. B Polym. Phys.* **15**:7 (1977), 1177–1188.

[Benveniste 1987] Y. Benveniste, "A new approach to the application of Mori–Tanaka's theory in composite materials", *Mech. Mater.* **6**:2 (1987), 147–157.

[Berlyand and Kozlov 1992] L. V. Berlyand and S. M. Kozlov, "Asymptotics of the homogenized moduli for the elastic chessboard composite", *Arch. Ration. Mech. An.* **118**:2 (1992), 95–112.

[Berlyand and Promislow 1995] L. V. Berlyand and K. Promislow, "Effective elastic moduli of soft medium with hard polygonal inclusions and external behavior of effective Poisson's ratio", *J. Elasticity* **40**:1 (1995), 45–73.

[Capaccio et al. 1976] G. Capaccio, T. A. Crompton, and I. M. Ward, "The drawing behavior of linear polyethylene, I: Rate of drawing as a function of polymer molecular weight and initial thermal treatment", *J. Polym. Sci. B Polym. Phys.* **14**:9 (1976), 1641–1658.

[Davidse et al. 1962] P. D. Davidse, H. I. Waterman, and J. B. Westerdijk, "Sound velocity and Young's modulus in polyethylene", *J. Polym. Sci.* **59** (1962), 389–400.

[Eshelby 1957] J. D. Eshelby, "The determination of the elastic field of an ellipsoidal inclusion, and related problems", *Proc. R. Soc. A* **241**:1226 (1957), 376–396.

[Flory 1969] P. J. Flory, *Statistical mechanics of chain molecules*, Oxford University Press, New York, 1969.

[Gavazzi and Lagoudas 1990] A. C. Gavazzi and D. C. Lagoudas, "On the numerical evaluation of the Eshelby's tensor and its application to elastoplastic fibrous composites", *Comput. Mech.* **7**:1 (1990), 13–19.

[Ghahremani 1977] F. Ghahremani, "Numerical evaluation of the stresses and strains in ellipsoidal inclusions in an anisotropic elastic material", *Mech. Res. Commun.* **4**:2 (1977), 89–91.

[Gray and McCrum 1969] R. W. Gray and N. G. McCrum, "Origin of the γ relaxations in polyethylene and polytetrafluoroethylene", *J. Polym. Sci.* **7**:8 (1969), 1329–1355.

[Hartmann and Jarzynski 1974] B. Hartmann and J. Jarzynski, "Immersion apparatus for ultrasonic measurements in polymers", *J. Acoust. Soc. Am.* **56**:5 (1974), 1469–1477.

[Hashin and Shtrikman 1963] Z. Hashin and S. Shtrikman, "A variational approach to the theory of the elastic behaviour of multiphase materials", *J. Mech. Phys. Solids* **11**:2 (1963), 127–140.

[Hermans 1967] J. J. Hermans, "The elastic properties of fiber-reinforced materials when the fibers are aligned", *P. K. Ned. Akad. Wetensc.* **B70** (1967), 1–9.

[Hill 1964] R. Hill, "Theory of mechanical properties of fibre-strengthened materials, I: Elastic behaviour", *J. Mech. Phys. Solids* **12**:4 (1964), 199–212.

[Hill 1965] R. Hill, "Theory of mechanical properties of fibre-strengthened materials, III: Self-consistent model", *J. Mech. Phys. Solids* **13**:4 (1965), 189–198.

[Hori and Nemat-Nasser 1993] M. Hori and S. Nemat-Nasser, "Double-inclusion and overall moduli of multi-phase composites", *Mech. Mater.* **14**:3 (1993), 189–206.

[Hu and Weng 2000] G. K. Hu and G. J. Weng, "The connections between the double-inclusion model and the Ponte Castaneda–Willis, Mori–Tanaka, and Kluster–Toksoz models", *Mech. Mater.* **32**:8 (2000), 495–503.

[Janzen 1992a] J. Janzen, "Crystalline elastic constants and macroscopic moduli of isotropic semi-crystalline polyethylene", *Polym. Eng. Sci.* **32**:17 (1992), 1255–1260.

[Janzen 1992b] J. Janzen, "Elastic moduli of semi-crystalline polyethylene compared with theoretical micromechanical models for composites", *Polym. Eng. Sci.* **32**:17 (1992), 1242–1254.

[Janzen 1997] J. Janzen, "Further refinement of the self-consistent model for the dependence of polyethylene elastic constants upon density", Paper presented at the ACS "Advances in Polyolefins" workshop (Napa Valley, CA), 1997.

[Jefferson et al. 2005] G. Jefferson, H. Garmestani, R. Tannenbaum, A. Gokhale, and E. Tadd, "Two-point probability distribution function analysis of co-polymer nano-composites", *Int. J. Plast.* **21**:1 (2005), 185–198.

[Jordens et al. 2000] K. Jordens, G. L. Wiles, J. Janzen, D. C. Rohlfing, and M. B. Welch, "The influence of molecular weight and thermal history on the thermal, rheological, and mechanical properties of metallocene catalyzed linear polyethylenes", *Polymer* **41**:19 (2000), 7175–7192.

[Lagakos et al. 1986] N. Lagakos, J. Jarzynski, J. B. Cole, and J. A. Bucaro, "Frequency and temperature dependence of elastic moduli of polymers", *J. Appl. Phys.* **59**:12 (1986), 4017–4031.

[de Langen et al. 2000] M. de Langen, H. Luigjes, and K. O. Prins, "High pressure NMR study of chain dynamics in orthorhombic phase of polyethylene", *Polymer* **41**:3 (2000), 1183–1191.

[Lee et al. 1993] B. J. Lee, D. M. Parks, and S. Ahzi, "Micromechanical modeling of large plastic deformation and texture evolution in semi-crystalline polymers", *J. Mech. Phys. Solids* **41**:10 (1993), 1651–1687.

[Lin and Garmestani 2000] S. Lin and H. Garmestani, "Statistical continuum mechanics analysis of an elastic two-isotropic-phase composite material", *Compos. B Eng.* **31**:1 (2000), 39–46.

[Molinari et al. 1987] A. Molinari, G. Canova, and S. Ahzi, "A self-consistent approach of the large deformation polycristal viscoplasticity", *Acta Metall.* **35**:12 (1987), 2983–2994.

[Mori and Tanaka 1973] T. Mori and K. Tanaka, "Average stress in matrix and average elastic energy of materials with misfitting inclusions", *Acta Metall.* **21**:5 (1973), 571–574.

[Nakayama et al. 1991] K. Nakayama, A. Furumiya, T. Okamoto, K. Yagi, A. Kaito, C. R. Choe, L. Wu, G. Zhang, L. Xiu, D. Liu, T. Masuda, and A. Nakajima, "Structure and mechanical propreties of ultra-high molecular weight polyethylene deformed near melting temperature", *Pure Appl. Chem.* **63** (1991), 1793–1804.

[Ponte Castaneda and Willis 1995] P. Ponte Castaneda and J. R. Willis, "The effect of spatial distribution on the effective behaviour of composite materials and cracked media", *J. Mech. Phys. Solids* **43**:12 (1995), 1919–1951.

[Takayanagi et al. 1966] M. Takayanagi, K. Imada, and T. Kajiyama, "Mechanical properties and fine structure of drawn polymers", *J. Polym. Sci. C Pol. Sym.* **15** (1966), 263–281.

[Wang 1973] T. T. Wang, "Morphology and mechanical properties of crystalline polymers, I: Transcrystalline polyethylene", *J. Appl. Phys.* **44**:5 (1973), 2218–2224.

[Ward 1985] I. M. Ward, *Mechanical properties of solid polymers*, Wiley, New York, 1985.

[Zehnder et al. 1996] M. M. Zehnder, A. A. Gusev, and U. W. Suter, "Predicting and understanding the elastic properties of polymers using atomistic simulation", *Rev. I. Fr. Petrol.* **51** (1996), 131–137.

[Zeller and Dederichs 1973] R. Zeller and P. H. Dederichs, "Elastic constants of polycrystals: basic research", *Phys. Status Solidi B* **55** (1973), 831–842.

SAID AHZI: ahzi@imfs.u-strasbg.fr
University Louis Pasteur, Institute of Fluid and Solid Mechanics, UMR 7507, 2 Rue Boussingault, 67000 Strasbourg, France

NADIA BAHLOULI: bahlouli@imsf.u-strasbg.fr
University Louis Pasteur, Institute of Fluid and Solid Mechanics, UMR 7507, 2 Rue Boussingault, 67000 Strasbourg, France

AHMED MAKRADI: makradi@imfs.u-strasbg.fr
University Louis Pasteur, Institute of Fluid and Solid Mechanics, UMR 7507, 2 Rue Boussingault, 67000 Strasbourg, France

SALIM BELOUETTAR: salim.belouettar
LTI, Research Center Henry Tudor, 70 Rue de Luxembourg, L-4221 Esch-sur-Alzette, Luxembourg